The Experimental Deformation Electron-Density Distributions of 4-Arylmethyleneamino-2,2,6,6-tetramethyl-1-piperidyloxyl (TEMPO) Radicals: Relations between Electron Densities and Intermolecular Interactions

Masanori Yasui, Eiji Kan-nari, Takayuki Ishida, Takashi Nogami, and Fujiko Iwasaki*

Department of Applied Physics and Chemistry, The University of Electro-Communications, Chofu, Tokyo 182-8585

(Received November 22, 1999)

Some of the 4-arylmethyleneamino-TEMPO radicals (TEMPO = 2,2,6,6-tetramethyl-1-piperidyloxyl), such as 4-(4-chlorobenzylideneamino)TEMPO (**1**) and 4-(benzylideneamino)TEMPO (**2**), showed intermolecular ferromagnetic interactions at an extremely low temperature. The experimental electron-density distributions of these compounds were investigated by the X-ray diffraction method. Intensity data were measured at 100 K up to $2\theta_{max}$(Mo $K\alpha$) = 120° and 95° for **1** and **2**, respectively. Deformation electron-density distributions were calculated from the structure factors after the refinements by the multipole expansion method. These electron-density distributions suggested that the unpaired electron of the O radical atom was not located on the O atom, but was rather located in the π^*-orbital of the N–O bond. Lone-pair densities of the radical O atom are located in the >N–O plane showing the sp^2 hybridization. From the crystal structures, it has been proposed that the ferromagnetic interactions are transferred through CH···O interactions between radical O atoms and β-H atoms of the neighboring TEMPO rings. The β-H atoms of the neighboring TEMPO rings contact with the O atom in the direction toward the π^*-orbital of the N–O bond, not in the direction of the lone-pair densities of the O atom. The present studies support the mechanism of the intermolecular ferromagnetic interactions through the β-H atoms. Studies of electron densities from the view point of the intermolecular interactions are important.

Organic magnetic substances are of great interest in materials science and physical chemistry. Some of the 4-arylmethyleneamino-TEMPO radicals (TEMPO = 2,2,6,6-tetramethyl-1-piperidyloxyl) showed intermolecular ferromagnetic interactions at an extremely low temperature, for example: 4-(4-Cl–C_6H_4)–CH=N–TEMPO (**1**), T_c = 0.4 K, θ = 0.7 K; 4-Ph–CH=N–TEMPO (**2**), T_c = 0.3 K, θ = 0.7 K (Scheme 1).[1,2] In the crystals of **1**, O atoms are arranged to form a pleated sheet parallel to the bc plane. The O···O distances in the sheet are 5.885(2) and 5.944(1) Å at 294 K. Within the sheet, O atoms contact with the H atoms of the CH_2 or CH_3 groups (β-H atoms) of the neighboring TEMPO rings, forming CH···O interactions.[3,4] Between sheets, the aryl groups of each sheet are arranged alternately face-to-face. In the case of **2**, two-dimensional O···O sheets are also constructed (5.617(2) and 6.145(1) Å at 296 K). Within the sheet, O atoms contact with the β-H atoms of the neighboring TEMPO rings. The packing mode of the aryl groups between sheets is a herringbone-type.[3,5] In the crystals of TEMPO radicals, the magnetic interactions are very weak, as shown from the extremely low magnetic transition temperatures and Weiss constants. It is difficult to point out the origin of the magnetic interactions exactly. Nevertheless, the sheet-like arrangements of O atoms and the intra-sheet interactions through β-H atoms of CH_2 or CH_3 groups of TEMPO rings are related to the mechanisms of the ferromagnetic interactions.[6,7] In order to shed light on the molecular interactions through β-H atoms, we investigated the electron-density distributions of these compounds by the X-ray diffraction method. Few experimental studies of electron-density distributions related to the intermolecular interactions of organic materials exhibiting physical properties are performed, although many studies on electron-density distributions of metal complexes and organic compounds have been reported.

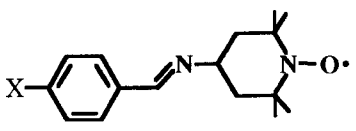

1 : X = Cl, **2** : X = H

Scheme 1.

Experimental

Crystals of **1** and **2** were recrystallized from methanol solutions. Crystal data and details of experimental conditions are listed in Table 1. The intensity data were measured on a Rigaku-AFC7R diffractometer at 100 K with an N_2-extraction gas-flow device. The $2\theta_{max}$ (Mo $K\alpha$) of the measurements are 120 and 95° for **1** and **2**, respectively. Absorption correction is applied for **1** using numerical method[8] but is not applied for **2**. Independent reflections observed with $I_0 > 2\sigma(I)$ were 8663 and 6050 out of 32459 and 28133 measured reflections for **1** and **2**, respectively.

Refinement of the Structures. Using room-temperature results as starting atomic parameters, structures were refined with

Table 1. Crystal Data and Experimental Condition

	1	**2**
Crystal data		
Chemical formula	$C_{16}H_{22}ClN_2O$	$C_{16}H_{23}N_2O$
Chemical formula weight	293.82	259.37
Weiss constant θ/K	0.7	0.7
Magnetic transition point T_c/K	0.4	0.3
Cell setting	Monoclinic	Monoclinic
Space group	$P2_1/c$	$P2_1/c$
a /Å	5.773(4)	12.577(1)
b /Å	24.130(4)	11.623(2)
c /Å	11.372(4)	10.823(2)
β /°	104.28(4)	110.85(1)
V /Å^3	1535(1)	1478.5(3)
Z	4	4
D_x /Mg m^{-3}	1.271	1.165
Radiation type	Mo $K\alpha$	Mo $K\alpha$
λ /Å	0.71073	0.71073
No. of reflections for cell parameters	25	25
θ range /°	12.8—17.4	12.9—15.2
μ /mm^{-1}	0.247	0.073
Temperature /K	100	100
Crystal form	Pillar	Prism
Color	Orange	Orange
Data collection		
Temperature /K	100	100
Crystal size /mm	0.10 × 0.15 × 0.52	0.35 × 0.35 × 0.2
Diffractometer	Rigaku AFC7R	Rigaku AFC7R
Data collection method	2θ–ω	2θ–ω
Absorption correction	Numerical	None
T_{min}	0.952	—
T_{max}	0.978	—
No. of measured reflections	32459	28133
No. of independent reflections	22780	13817
No. of reflections with $I > 2.0\sigma(I)$	8663	6050
R_{int}	0.0369	0.0581
θ_{max} /°	60.0	47.5
Range of h, k, l	0—13, −41—58, −27—26	0—26, −24—24, −22—20
No. of standard reflections	3 (Every 150 refs.)	3(Every 150 refs.)
Intensity decay (%)	2.11	3.40
Decay correction	None	Applied

full-matrix least-squares methods using the program SHELXL-97.[9] R-factors converged to 0.0451 and 0.0499 for 8663 and 6050 reflections ($I_0 > 2\sigma(I)$) for **1** and **2**, respectively. Atomic positions and temperature factors of non-H atoms were refined using reflections with $\sin\theta/\lambda > 0.5$, to avoid the effect of the valence electrons on the atomic scattering factors. At this stage, R values were 0.0501 and 0.0656 for 7208 and 5199 reflections for **1** and **2**, respectively. With these atomic positions and temperature factors held fixed, multipole population parameters P_{lm} of each atom were refined using the multipole expansion atomic scattering factors[10—13] by the program MOLLY 5.[10] A hexadecapole expansion was applied to Cl and an octapole expansion to other non-H atoms. For **1**, the extraction-contraction coefficients, κ', and the extinction parameter are refined. After refinements with population parameters, positional parameters and temperature factors, the final R values were 0.0411 and 0.0453 for 9026 and 6608 reflections ($F_o > 3\sigma(F)$) for **1** and **2**, respectively. Details of refinements were listed in Table 2. Scattering factors of free spherical atoms, core and valence electrons were taken from "International Tables for X-ray Crystallography".[14] Crystallographic data have been deposited at the CCDC, 12 Union Road, Cambridge CB2 1EZ, UK and copies can be obtained on request, free of charge, by quoting the publication citation and the deposition numbers 143538-143539.

Results and Discussion

Atomic parameters obtained from the final refinement are listed in Table 3.[15] ORTEP drawings[16] of the molecules are shown in Fig. 1 with atom numbering. Bond lengths and angles are listed in Table 4. The relationships between the

Table 2. Details of Refinements

	1	2
Conventional refinement		
Program	SHELXL-97	SHELXL-97
Refinement on	F^2	F^2
No. of reflections with $I > 2\sigma(I)$	8663	6050
$R\,[I > 2\sigma(I)]$	0.0451	0.0499
$wR(F^2)$	0.1593	0.1729
S	0.924	0.967
No. of parameters used	269	195
H-atom treatment	All refined	Riding model
Weighting scheme[a] a, b	0.0641, 0.0	0.0764, 0.0
$(\Delta/\sigma)_{max}$	0.001	0.009
ρ_{max} / eÅ^{-3}	0.59	0.40
ρ_{min} / eÅ^{-3}	−0.38	−0.34
High order refinement		
Program	SHELXL-97	MOLLY-5
Refinement on	F^2	F
H-atom treatment	Riding model	Fixed
Lower limit of sin θ/λ	0.5	0.5
No. of reflections	7208	5199
No. of parameters used	181	172
R	0.0501	0.0656
Multipole refinement		
Program	MOLLY-5	MOLLY-5
No. of reflections with $F_o > 3.0\sigma(F)$	9026	6608
Octapole refinement		
No. of parameters used	325	305
R	0.0430	0.0507
Hexadecapole refinement		
No. of parameters used	331	—
R	0.0426	—
Refinement including atomic positions		
No. of parameters used	514	476
R	0.0411	0.0453
wR	0.0436	0.0390
Weighting scheme	$1/(\sigma^2(F_o) + 0.00012F_o^2)$	$1/(\sigma^2(F_o) + 0.00003F_o^2)$
S	1.135	1.219
$(\Delta/\sigma)_{max}$	0.06	0.001
Extinction method	Isotropic type I Gaussian	None
Extinction parameter $g/10^4$	0.003(7)	—
ρ_{max} / eÅ^{-3}	0.296	0.242
ρ_{min} / eÅ^{-3}	−0.277	−0.273

a) $w = 1/[\sigma^2(F_o^2) + (aP)^2 + bP]$, where $P = (F_o^2 + 2F_c^2)/3$.

radical O atoms and the β-H atoms (H atoms attached to C3, C21, C22, C5, C61, and C62) of the neighboring TEMPO rings are shown in Table 5 and Fig. 2. At 100 K cell parameters of **1** were compressed by 1.90, 1.18, and 0.22% for a, b, and c axes, respectively. The corresponding values of **2** are 0.86, 1.00, and 1.82%. The directions of the largest shortening correspond to the shortest O···O directions for both **1** and **2**. The radical N–O lengths at 100 K are 1.2827(14) Å for **1** and 1.2815(15) Å for **2**, which are slightly shorter than those at 100 K before the multipole refinements (1.2860(8) and 1.2888(11) Å for **1** and **2**, respectively). In the conventional refinements with the spherical atomic scattering factors, the apparent positions of the O atoms may be affected by the contributions of the lone-pair electron densities.

The deformation maps and the residual maps are shown in Figs. 3 and 4, respectively. The deformation maps,

$$\Delta\rho = \rho[\text{obs}] - \rho[\text{calc, spherical-atom}]$$

showed the bonding electrons between C–C and C–N bonds

Table 3. Fractional Atomic Coordinates and Equivalent Isotropic Temperature Factors (B_{eq}) for Non-H Atoms $B_{eq} = (4/3)\pi^2 \sum_i \sum_j U_{ij} \boldsymbol{a}_i^* \boldsymbol{a}_j^* \boldsymbol{a}_i \boldsymbol{a}_j$

Atom	x	y	z	B_{eq}/Å^2
(a) **1**				
Cl1	0.44089(5)	0.005361(9)	−0.32663(2)	1.946(5)
O1	−0.21696(19)	0.21690(4)	0.50580(9)	1.541(17)
N1	−0.10559(14)	0.19501(3)	0.43278(7)	1.096(12)
N2	0.18702(15)	0.11716(4)	0.17211(8)	1.287(14)
C2	−0.04455(15)	0.23299(3)	0.34118(7)	1.105(12)
C3	0.01939(14)	0.19899(3)	0.23952(7)	1.152(13)
C4	0.18236(14)	0.14907(3)	0.28105(7)	1.145(13)
C5	0.07411(15)	0.11244(3)	0.36331(7)	1.285(14)
C6	0.02782(15)	0.14245(3)	0.47414(7)	1.158(13)
C7	0.37393(15)	0.11935(4)	0.13224(7)	1.226(13)
C11	0.39080(15)	0.09075(3)	0.01993(7)	1.144(13)
C12	0.21672(17)	0.05248(4)	−0.03620(9)	1.510(16)
C13	0.23030(19)	0.02598(4)	−0.14293(9)	1.721(18)
C14	0.42059(17)	0.03857(4)	−0.19365(8)	1.353(15)
C15	0.59482(18)	0.07672(4)	−0.14044(8)	1.568(17)
C16	0.58065(17)	0.10235(4)	−0.03228(8)	1.543(16)
C21	0.15935(18)	0.27202(4)	0.40325(8)	1.564(16)
C22	−0.26745(17)	0.26776(4)	0.28665(8)	1.534(16)
C61	0.26063(17)	0.15581(4)	0.56911(8)	1.568(16)
C62	−0.13099(18)	0.10607(4)	0.53217(9)	1.611(17)
(b) **2**				
O1	0.45295(12)	0.80060(10)	0.29619(13)	2.07(3)
N1	0.40011(9)	0.71703(8)	0.22263(10)	1.467(19)
N2	0.22557(10)	0.43224(9)	−0.00318(10)	1.64(2)
C2	0.47320(9)	0.62303(9)	0.20131(9)	1.550(19)
C3	0.40136(9)	0.54042(8)	0.09326(9)	1.546(18)
C4	0.28929(9)	0.50555(8)	0.10803(9)	1.516(18)
C5	0.22008(8)	0.61414(8)	0.10325(9)	1.531(18)
C6	0.27954(9)	0.70122(8)	0.21244(9)	1.499(19)
C7	0.21216(8)	0.32772(8)	0.02209(9)	1.568(19)
C11	0.14802(8)	0.24454(8)	−0.08008(10)	1.518(19)
C12	0.09896(9)	0.27623(9)	−0.21344(10)	1.71(2)
C13	0.03555(10)	0.19670(10)	−0.30663(10)	1.89(2)
C14	0.02029(10)	0.08494(10)	−0.26873(12)	1.93(2)
C15	0.06943(10)	0.05283(9)	−0.13645(13)	1.97(3)
C16	0.13320(10)	0.13198(9)	−0.04276(11)	1.81(2)
C21	0.53219(10)	0.56117(10)	0.33343(11)	2.19(2)
C22	0.56256(10)	0.67985(12)	0.15493(12)	2.30(3)
C61	0.27686(10)	0.66226(10)	0.34685(10)	2.01(2)
C62	0.22007(10)	0.81807(9)	0.17697(11)	2.03(2)

and the lone-paired electrons of the O atoms. On the contrast, only noise peaks were shown in the multipole residual maps,

$$\Delta\rho = \rho[\text{obs}] - \rho[\text{calc, multipole-atom}].$$

This means that the structures were refined reasonably by the multipole expansion method.

Figures 5 and 6 show model-deformation maps,

$$\Delta\rho = \rho[\text{calc, multipole-atom}] - \rho[\text{calc, spherical-atom}]$$

Table 4. Selected Bond Lengths (l) and Angles (θ) of Non-H Atoms

	1	**2**
Lengths	l/Å	l/Å
Cl1–C14	1.7408(10)	
O1–N1	1.2827(14)	1.2815(15)
N1–C2	1.4934(12)	1.4977(15)
N1–C6	1.4980(10)	1.4921(16)
N2–C4	1.4644(12)	1.4595(13)
N2–C7	1.2705(13)	1.2696(14)
C2–C3	1.5351(11)	1.5341(13)
C3–C4	1.5299(10)	1.5287(17)
C4–C5	1.5281(12)	1.5236(14)
C5–C6	1.5331(12)	1.5333(12)
C7–C11	1.4759(12)	1.4741(12)
Angles	θ/°	θ/°
O1–N1–C2	116.17(8)	115.95(11)
O1–N1–C6	116.51(8)	115.34(11)
C2–N1–C6	123.16(7)	124.20(10)
C4–N2–C7	118.33(9)	117.19(11)
N1–C2–C3	109.84(7)	110.29(9)
C2–C3–C4	115.61(7)	113.64(9)
N2–C4–C3	106.92(7)	108.94(10)
N2–C4–C5	108.04(7)	108.44(9)
C3–C4–C5	109.34(7)	108.29(9)
C4–C5–C6	114.25(7)	113.87(9)
N1–C6–C5	108.79(7)	110.02(9)
N2–C7–C11	122.18(9)	123.03(10)
C7–C11–C12	120.70(8)	121.52(10)
C7–C11–C16	120.01(8)	119.31(10)

Table 5. Selected Intermolecular Distances (l) Related to the O Radical Atoms and the Distance (l) between the Phenyl Planes

1		**2**	
Lengths	l/Å	Lengths	l/Å
O1···O1^{i}	5.7732(6)	O1···O1^{i}	5.538(3)
O1···O1^{ii}	5.9062(19)	O1···O1^{ii}	6.084(2)
O1···C3^{ii}	3.3549(11)	O1···C3^{ii}	3.3163(15)
O1···C22^{ii}	3.2988(14)	O1···C21^{ii}	3.3707(17)
O1···H61^{i}	2.68	O1···H32^{ii}	2.43
O1···H21^{i}	2.80	O1···H23^{ii}	2.64
O1···H26^{ii}	2.47	O1···H24^{i}	2.80
Ph···Ph^{iii}	3.568(1)		
Symmetry code:		Symmetry code:	
i = $x-1, y, z$;		i = $x, 3/2-y, 1/2+z$;	
ii = $x, 1/2-y, 1/2+z$;		ii = $1-x, 1/2+y, 1/2-z$.	
iii = $1-x, -y, -z$.			

for **1** and **2**, respectively. To plot model deformation maps, structure factors were calculated up to $\sin\theta/\lambda = 1.2185$ ($2\theta = 120°$), including non-observed indices. Model deformation maps clearly show the features of deformation densities because of the elimination of experimental errors

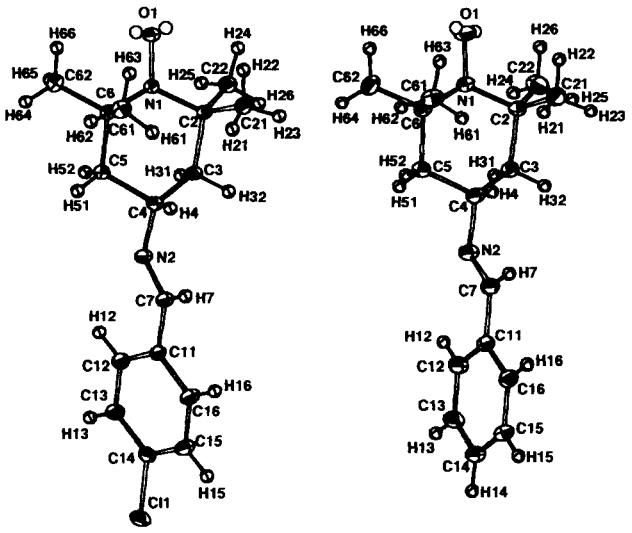

Fig. 1. ORTEP drawings with the atom-numbering. The thermal ellipsoids for non-H atoms are drawn at 50% probability and the H atoms are drawn as spheres with a radius of 0.1 Å. Lone-pair electrons of the O atoms are shown as small open circles. (a) **1** and (b) **2**.

and cut-off effects of Fourier summation. In the model deformation maps, shapes and magnitudes of peaks between N–C and C–C bonds show normal features. Lone pairs of the radical O1 atoms of **1** and **2** are clearly observed in the section of the O1–C2–C6 planes (Figs. 5a and 6a, respectively). The angles of L1–O1–L2, where L1 and L2 denote the peak positions of electron densities assinged to lone-pair electrons, are 145 and 153° for **1** and **2**, respectively. From the section perpendicular to the O(1)–C(2)–C6 plane through the N–O bond, no peaks are observed up and down side of the N–O bond at the N1 and O1 atoms (Figs. 5b and 6b, respectively). These facts show the character of the sp^2 hybridization of the O atom.

In the section of the phenyl plane of **1** (Fig. 5c), the peak of the bonding electron of C–Cl is not observed. The electron densities of the free Cl atom is originally anisotopic, where the contributions of only one electron in C–Cl bond and four electrons in 3p orbitals deviate from the spherical densities. Thus the difference densities are much reduced at the C–Cl bond in the model deformation map.

In order to clarify the bonding electrons of C–Cl and N–O groups, we also calculated the structure factors using the oriented atom model (OAM),[17,18] not the spherical atom model. In this model, five electrons of the Cl atom belonging to the p-orbitals are treated anisotopically; one is in the direction of the Cl–C bond, two are in the direction perpendicular to the phenyl plane, and two are in the direction perpendicular to these two directions. The electrons of N and O atoms are treated as sp^2 hybridization. In the p_z orbital, two and one electrons are located for N and O atoms, respectively. The lone-pair densities should disappear in the difference densities,

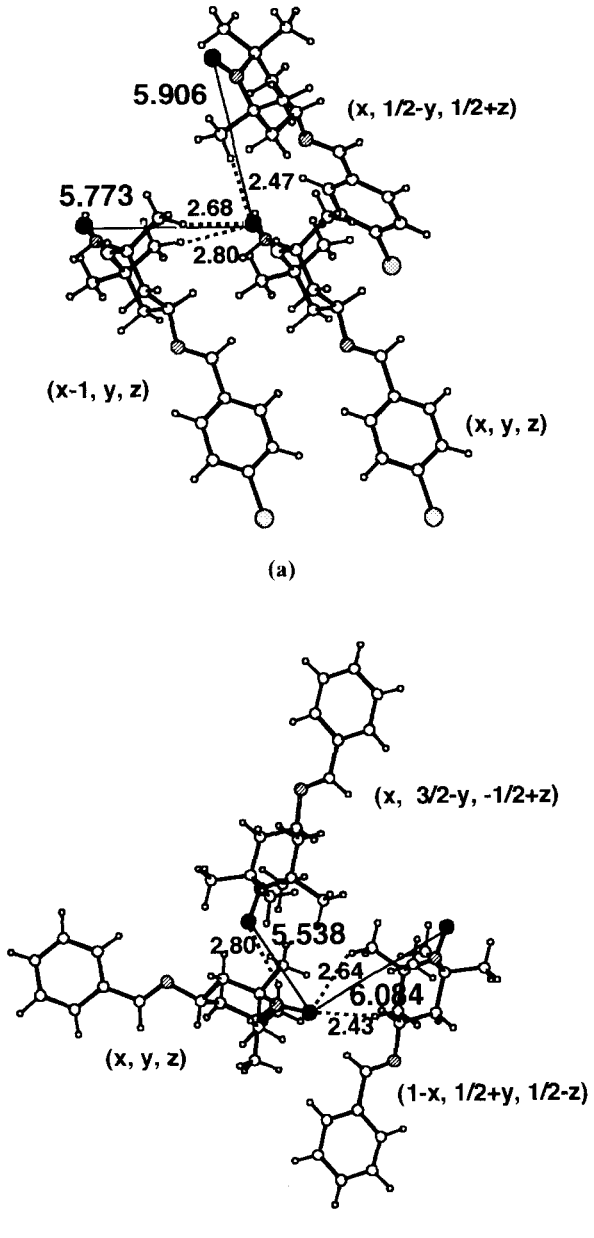

Fig. 2. Relationships between O atoms and β-H atoms of the neighboring TEMPO rings. (a) **1** and (b) **2**.

$$\Delta\rho = \rho[\text{calc, multipole-atom}] - \rho[\text{calc, OAM}].$$

These maps of **1** and **2** are shown in Fig. 7. The bonding electron densities are clearly shown in the C–Cl bond as shown in Fig. 7a. Negative peaks appeared at the N1 atom in the section perpendicular to the O1–C2–C6 plane through the N–O bond in Figs. 7c and 7e. This means that the lone-pair electrons of the N atom not observed in Figs. 5 and 6, are used to make the π and π^* orbital of the N–O bond.

The contacts between the lone pairs of the O atoms and β-H atoms of the neighboring molecules are shown in Fig. 8. The β-H atoms contact with the O atom in the direction toward the π^* orbital of the N–O bond.

To summarize the molecular interactions from the defor-

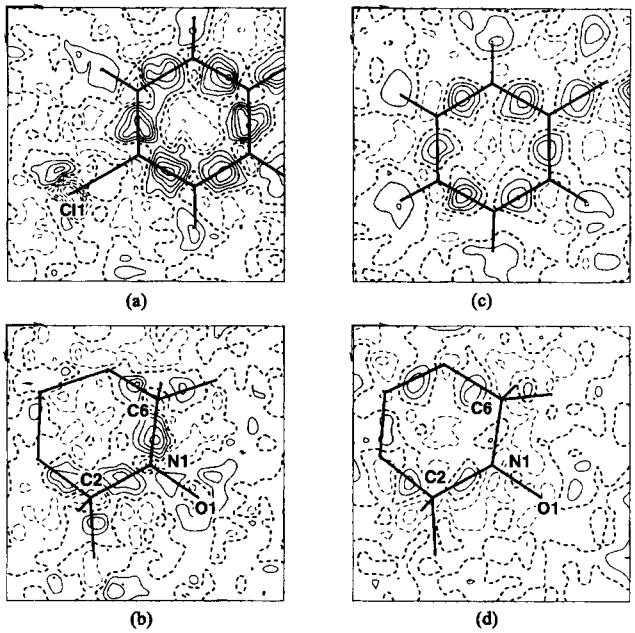

Fig. 3. Deformation maps, $\Delta\rho = \rho$[obs] $- \rho$[calc, spherical-atom].(a) Section of the phenyl plane of **1**. (b) Section of the O1–C2–C6 plane of **1**. (c) Section of the phenyl plane of **2**. (d) Section of the O1–C2–C6 plane of **2**. Contour lines are at 0.1 e Å^{-3} intervals. Lines represent positive (solid), zero (thick dotted), and negative (thin dotted) contours. (Same definition is used in all maps.)

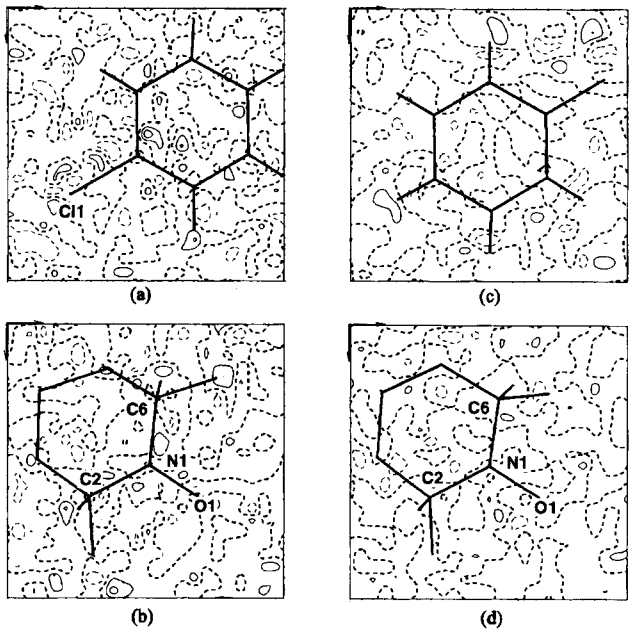

Fig. 4. Residual maps, $\Delta\rho = \rho$[obs] $- \rho$[calc, multipole-atom].(a) Section of the phenyl plane of **1**. (b) Section of the O1–C2–C6 plane of **1**. (c) Section of the phenyl plane of **2**. (d) Section of the O1–C2–C6 plane of **2**.

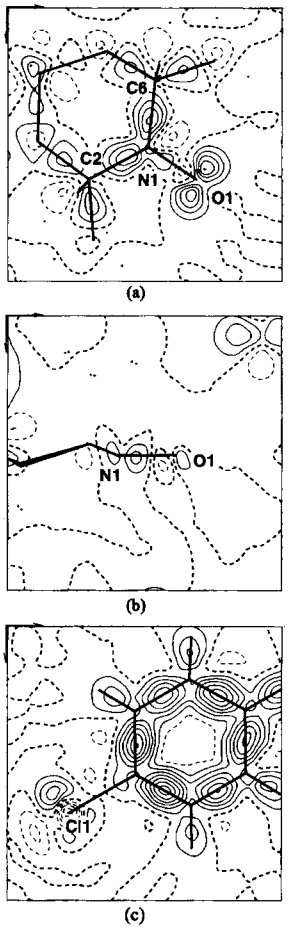

Fig. 5. Model-deformation maps, $\Delta\rho = \rho$[calc, multipole-atom] $- \rho$[calc, spherical-atom], of **1**. (a) Section of the O1–C2–C6 plane. (b) Section perpendicular to the O1–C2–C6 plane through the N–O bond. (c) Section of the phenyl plane.

mation electron-densities: (1) Lone pairs of the radical O atoms are located in the >N–O plane, which shows the sp^2 hybridization of O atom. (2) An unpaired electron of the O atom is not located on the O atom, but is located in the π^*-orbital of the N–O bond. (3) The β-H atoms of the neighboring TEMPO rings contact with the O atom in the directions towards the π^*-orbital. These facts support the mechanism of the intermolecular ferromagnetic interactions through the β-H atoms.[6,7]

Usually, weak intermolecular interactions work anisotopically in the crystals and these interactions often control the physical properties of the organic crystals. It is interesting and important to study electron densities from the view point of the intermolecular interactions.

This work was supported in part by a Grant-in-Aid for Scientific Research No. 08454180 from the Ministry of Education, Science, Sports and Culture.

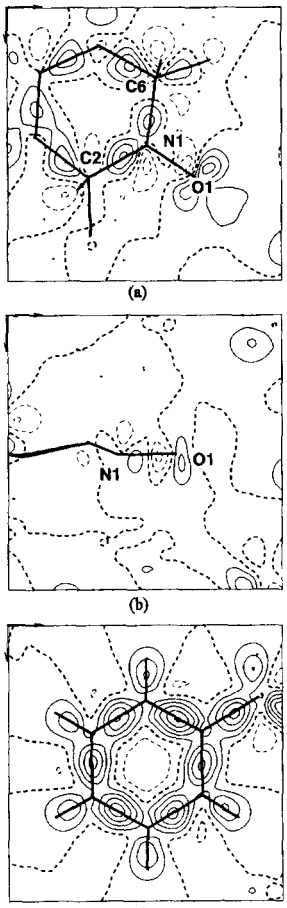

Fig. 6. Model-deformation maps, $\Delta\rho = \rho$[calc, multipole-atom] $- \rho$[calc, spherical-atom], of **2**. (a) Section of the O1–C2–C6 plane. (b) Section perpendicular to the O1–C2–C6 plane through the N–O bond. (c) Section of the phenyl plane.

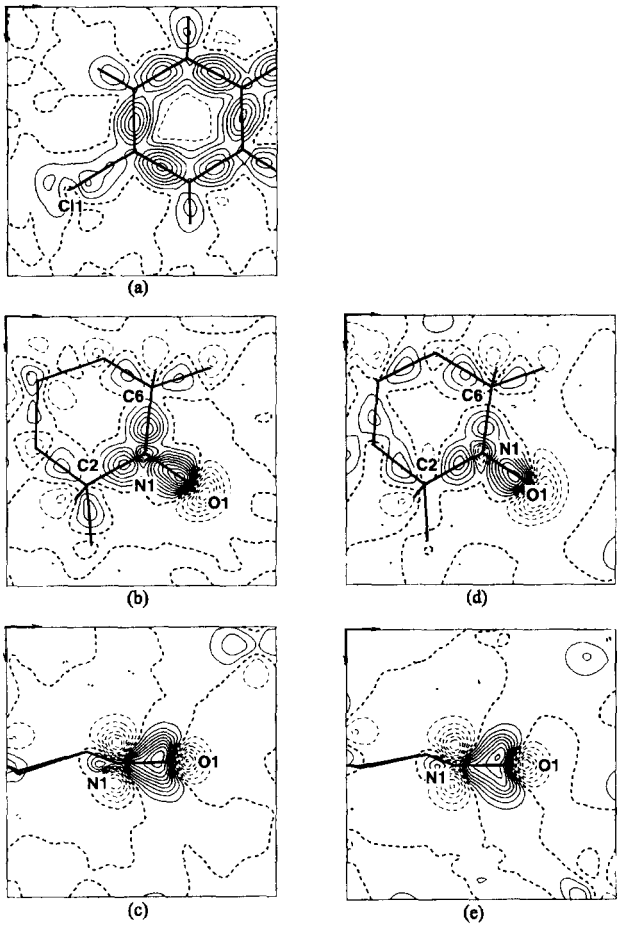

Fig. 7. Model-deformation maps, $\Delta\rho = \rho$[calc, multipole-atom] $- \rho$[calc, OAM]. (a) Section of the phenyl plane of **1**. (b) Section of the O1–C2–C6 plane of **1**. (c) Section perpendicular to the O1–C2–C6 plane through the N–O bond of **1**. (d) Section of the O1–C2–C6 plane of **2**. (e) Section perpendicular to the O1–C2–C6 plane through the N–O bond of **2**.

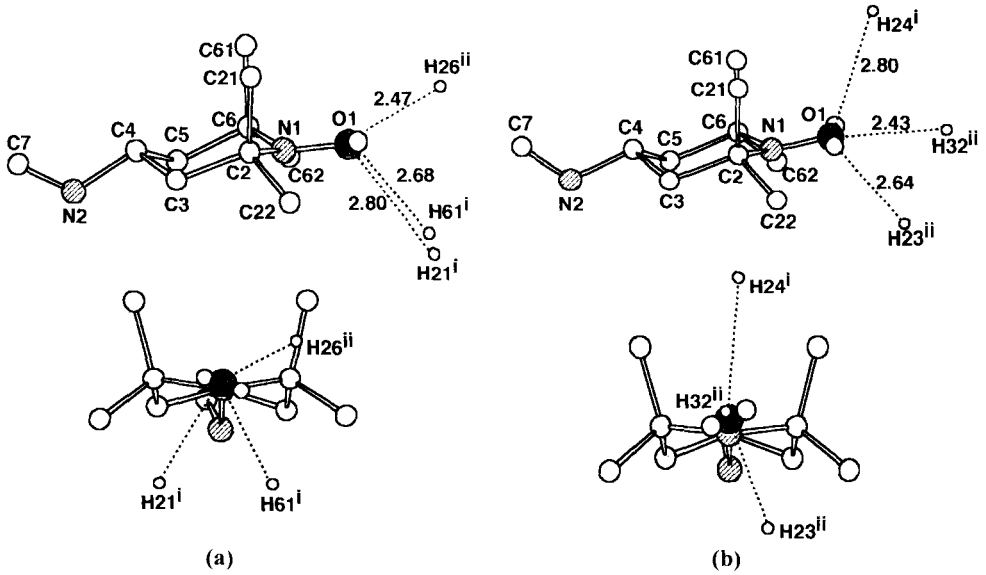

Fig. 8. Relationships between lone-pair electrons of O atoms and β-H atoms of the neighboring TEMPO rings. (a) **1** (Symmetry code: i = $x-1, y, z$; ii = $x, 1/2-y, 1/2+z$) and (b) **2** (Symmetry code: i = $x, 3/2-y, 1/2+z$; ii = $1-x, 1/2+y, 1/2-z$).

References

1 T. Nogami, K. Tomioka, T. Ishida, H. Yoshikawa, M. Yasui, F. Iwasaki, H. Iwamura, N. Takeda, and M. Ishikawa, *Chem. Lett.*, **1994**, 29.

2 T. Nogami, T. Ishida, H. Tsuboi, H. Yoshikawa, H. Yamamoto, M. Yasui, F. Iwasaki, H. Iwamura, N. Takeda, and M. Ishikawa, *Chem. Lett.*, **1995**, 635.

3 M. Yasui, J. H. Yoshikawa, H. Yamamoto, T. Ishida, T. Nogami, and F. Iwasaki, *Mol. Cryst. Liq. Cryst.*, **279**, 77 (1996).

4 F. Iwasaki, J. H. Yoshikawa, H. Yamamoto, K. Takada, E. Kannari, M. Yasui, T. Ishida, and T. Nogami, *Acta Crystallogr., Sect. B*, **B55**, 231 (1999).

5 F. Iwasaki, J. H. Yoshikawa, H. Yamamoto, K. Takada, E. Kannari, M. Yasui, T. Ishida, and T. Nogami, *Acta Crystallogr., Sect. B*, **B55**, 1057 (1999).

6 T. Nogami, T. Ishida, M. Yasui, F. Iwasaki, N. Takeda, M. Ishikawa, T. Kawakami, and K. Yamaguchi, *Bull. Chem. Soc. Jpn.*, **69**, 1841 (1996).

7 T. Kawakami, A. Oda, S. Takeda, W. Mori, T. Ishida, M. Yasui, F. Iwasaki, T. Nogami, and K. Yamaguchi, *Mol. Cryst. Liq. Cryst.*, **306**, 141 (1997).

8 P. Coppens, L. Leiserowitz, and D. Rabinovich, *Acta Crystallogr.*, **18**, 1035 (1965).

9 G. M. Sheldrick, "SHELXL-97. Program for crystal structure determination," University of Göttingen, Germany (1997).

10 N. K. Hansen and P. Coppens, *Acta Crystallogr., Sect. A*, **A34**, 909 (1978).

11 P. Coppens and M. B. Hall, "Electron Distributions and the Chemical Bond," Plenum Press, New York (1982).

12 T. Ito, *J. Cryst. Soc. Jpn.*, **27**, 270 (1985).

13 In the multipole expansion method atomic density is defined as

$$\rho_{\mathrm{atom}}(\boldsymbol{r}) = P_{\mathrm{c}}\rho_{\mathrm{core}}(r) + P_{\mathrm{v}}\kappa'^{3}\rho_{\mathrm{valence}}(\kappa' r) + \sum \kappa''^{3} R_l(\kappa'' r) \sum P_{lm} y_{lm}(\boldsymbol{r}/r),$$

where P_{c}, P_{v}, and P_{lm} are population coefficients, κ' and κ'' are expansion-contraction coefficients, y_{lm} is a real spherical harmonic function and R_l is a STO radial function shown as

$$R_l(r) = N r^{nl} \exp(-\xi r).$$

The corresponding atomic scattering factor is expressed as

$$f(\boldsymbol{h}) = P_{\mathrm{c}} f_{\mathrm{core}}(h) + P_{\mathrm{v}} f_{\mathrm{val}}(h/\kappa') + \sum f_l(h/\kappa'') \sum P_{lm} y_{lm}(\boldsymbol{h}/h).$$

14 "International Tables for X-Ray Crystallography," Vol. C, Kynoch Press, Birmingham (Present distributor D. Reidel, Dordrecht) (1992).

15 Lists of structure factors after multipole refinement, anisotropic temperature factors for non-H atoms, atomic parameters for H-atoms, multipole coefficients of all non-H atoms, all bond lengths and angles, figures of local Cartesian coordinates for the multipole refinement, deformation maps, and residual maps have been deposited as Document No. 73035 at the Office of the Editor of Bull. Chem. Soc. Jpn.

16 C. K. Johnson, "ORTEP II, Report ORNL-5138," Oak Ridge National Laboratory, Tennessee, USA (1976).

17 W. H. E. Schwarz, P. Valtazanos, and K. Ruedenberg, *Theor. Chim. Acta*, **68**, 471 (1985).

18 H. Takazawa, S. Ohba, and Y. Saito, *Acta Crystallogr., Sect. B*, **B45**, 432 (1989).